SYNTHESIS OF A BETA-SHEET ANALOG DERIVED FROM A 26-ATOM MACROCYCLE INCORPORATING LEUCINE

by

Luke Homfeldt

Submitted in partial fulfillment for Departmental Honors

in the Department of Chemistry and Biochemistry

Texas Christian University

Fort Worth, Texas

May 6, 2024

SYNTHESIS OF A BETA-SHEET ANALOG DERIVED FROM A 26-ATOM MACROCYCLE INCORPORATING LEUCINE

Project Approved:

Supervising Professor: Eric Simanek, Ph. D

Department of Chemistry and Biochemistry

David Minter, Ph. D

Department of Chemistry and Biochemistry

Giri Akkaraju, Ph. D

Department of Biology

ABSTRACT

Pharmaceutical development maintains a disproportionate focus on the synthesis of small molecules. This emphasis is based on historical research about bioavailability of molecules and the position that small molecule synthesis is cheaper and more efficient than the synthesis of large molecules. Macrocycles challenge these beliefs vis-a-vis the viability of large molecule pharmaceuticals. With availability in a simple three step process, macrocycles demonstrate the potential to be bioavailable and maintain biologically useful conformations in solution, representing a new frontier in pharmaceutical development. The previous synthesis of the 26-atom **G-G** macrocycle indicates that these molecules can maintain a *beta*-sheet like structure which could be utilized in antagonizing protein-protein interactions like the formation of *beta*-amyloid plaques in Alzheimer's disease.[1]

The synthesis of the leucine 26-atom macrocycle in this project investigates how the addition of leucine, a bulky hydrophobic amino acid, affects the formation of the planar structure as adopted by the **G-G** macrocycle. The macrocycle is obtained through a three-step reaction pathway. BOC-hydrazine, leucine, and dimethylamine (DMA) are added sequentially to a triazine core in a one-pot reaction. This acid then has a four-carbon acetal group installed using conventional coupling reagents to create the monomer. Dimerization of monomer is induced using a 1:1 mixture of dichloromethane (DCM) and trifluoracetic acid (TFA). Upon evaporation of solvent, this reaction is found to be qualitative in its yield of macrocycle.

Both ^{13}C and ^{1}H NMR spectra are used to confirm the resulting macrocycle's formation. COSY and rOesy two-dimensional NMR are utilized to assign structure. Downfield shifts of critical resonances in the ^{1}H NMR spectra confirm that the macrocycle adopts a *beta*-sheet conformation.

ACKNOWLEDGEMENTS

I would like to thank everyone who made this thesis come to light. I would like to specifically highlight Dr. Eric Simanek for bringing me into the Simanek lab group and facilitating my growth as a researcher. I would also like to thank all the graduate students: Alexander Menke, Casey Patterson-Gardner, Gretel Stokes, and Liam Claton. Even with their intense schedules each of these individuals invested their time in my learning. My research experience would not be the same without them. Thank you to Dr. David Minter and Dr. Giri Akkaraju, for encouraging me and helping me achieve all my goals, making me a better student every day. To the professors in the Department of Biochemistry and Chemistry, thank you for all the lessons and insight on both chemistry and life. To my friends and family, thank you for the unending love and support that helped propel me forward. Thank you to the John V. Roach Honors College for providing the opportunity for me to write this thesis and share my work. Lastly, thank you to the National Institute of Health and the Robert A. Welch Foundation for helping fund this project.

TABLE OF CONTENTS

TERMINOLOGY AND ABBREVIATIONS

Abbreviation	Full Term
BOC	tert-butyl carbazate
COSY	homonuclear correlation spectroscopy
DCM	dichloromethane
DIPEA	diisopropylethylamine
DMA	dimethylamine
DMSO	dimethyl sulfoxide
DMSO-d_6	deuterated dimethyl sulfoxide
HBTU	2-(1H-benzotriazole-1-yl)-1,1,3,3-tetramethyuronium hexafluorophosphate
HPLC	high performance liquid chromatography
MeOH	methanol
NaOH	sodium hydroxide
NMR	nuclear magnetic resonance spectroscopy
ppm	parts-per-million
rOesy	rotating frame Overhauser effect spectroscopy
TFA	trifluoroacetic acid
THF	tetrahydrofuran
TLC	thin layer chromatography

FIGURES AND SCHEMES

INTRODUCTION

Large, cyclic molecules have been grossly underrepresented in pharmaceutical research. Apart from certain naturally occurring drugs such as cyclosporin and erythromycin there are few drugs with cyclic structures that have garnered attention and are thought to be pharmaceutically viable.[2] This belief is unfortunate as large cyclic molecules possess unique structures that showcase the potential for interacting with intracellular targets in diverse and dynamic ways including the inhibition of protein-protein interactions (PPI) which can impact signal transduction and protein aggregation.

Triazine macrocycles challenge the traditional issues of large molecule pharmaceuticals. They can be synthesized through a simple pathway in high product yields. The synthesis of macrocycles utilizing triazine as the foundational molecule can result in a high yield of product after acetylation and acidification.[3] The macrocycles synthesized using this pathway are excellent model pharmaceuticals due to their easily-modifiable structure. These molecules offer insight into the folding, structure, and permeability of other macrocycles. The ability to exchange one or more of the four building blocks used in synthesis: the BOC-protected hydrazine, amino acid, auxiliary group, and acetal lends itself to the creation of a diverse array of molecules. By altering these groups, data can be collected and assessed to understand what modifications are more conducive to a pharmaceutical model. Analysis of the molecular structure is of particular interest as macrocycles have been observed to possess an array of conformations.

Structure can be assessed by determining how distant domains of the molecule sense each other in what is called a rOe interaction. Specifically, a rOesy NMR experiment reveals proton-proton

interactions occurring through space.[4.] Identification of these interactions show that 24-atom macrocycles exhibit dynamic motion and a folded conformation. Determining the conformation of the 26-atom macrocycle described here is one of the goals of this research. These conformational states are thought to play a role in the noted potential bioavailability of the macrocycles.

For a molecule to be bioavailable it must be able to pass through the cell membrane from the aqueous environment of the body. This behavior is captured in a metric called the water/octanol coefficient; also known as logP. By utilizing high performance liquid chromatography (HPLC), it has been found that certain modifications of the 24-atom macrocycles allow for logP values that are within the range for bioavailability, which are seen in traditional small molecule pharmaceuticals.[3] These predictions put macrocycles in conflict with the *Rule of Five* that traditionally dictates understanding of small molecule bioavailability and cell membrane permeability.[5] This finding underscores how much remains to be understood about pharmaceutical design, especially when it comes to the structure and composition of large cyclic molecules.

The size of the macrocycle plays an influential role in the resulting structure. An exploration of this property demonstrates the wide variety of structures that are made available in macrocycles.[1] This alteration in size comes from variance in the length of the installed acetal group, which can vary from 2-5 carbons. While smaller ring sizes between 22 and 24 atoms displayed folded structures, larger 26 and 28 atom macrocycles demonstrated planar and “crinkled” conformations respectively.[1] Of particular interest is the 26-atom macrocycle, **G-G,** which showed a planar conformation by X-ray crystallography (**Figure 1).**[1]

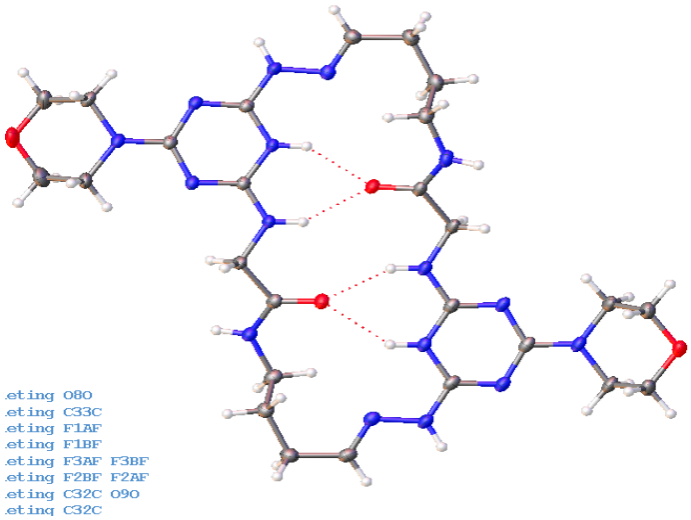

Figure 1. Macrocycle **G-G**, a 26-atom cyclic molecule

This planar structure is similar to that of a *beta*-sheet conformation in the secondary structure of proteins. With a network of hydrogen bonds stabilizing the shape of the molecule. These hydrogen bonding interactions are thought to be the primary reason for the planar conformation. The logP of similar 24-atom macrocycles falls within an acceptable range to cross membranes, and accordingly, these *beta*-sheet analogs could show promise in being able to inhibit or break apart protein aggregates and protein-protein interactions (PPIs) that are contingent on *beta*-sheet binding. This behavior could be valuable in preventing or treating the onset of certain conditions, such as Alzheimer's disease which results from the stacking of misfolded *beta*-amyloid proteins. Because PPIs involve large featureless binding areas, inhibition of this stacking could be possible through the usage of protein mimics with analogous structures.[6] Macrocycle **G-G** indicates that the *beta* conformation of these macrocycles can be adopted (**Figure 1**) but it is still unknown whether bulky aliphatic amino acid substitutions will be detrimental to the structure of the 26-atom macrocycle.[5]

The motivation for the synthesis of the 26-atom macrocycle, **L-L**, is to identify whether the *beta*-sheet structure of **G-G** is conserved after substitution with large non-polar amino acid side chains.

The synthesis of **L-L** relies on the dimerization of **L**-monomer (**Scheme 1)**. The addition and subsequent evaporation of trifluoroacetic acid (TFA) and dichloromethane (DCM) from the monomer results in the dimerization and full cyclization of the macrocycle in a quantitative yield (**Scheme 1)**.

Scheme 1. The **L** monomer dimerization to **L-L** macrocycle

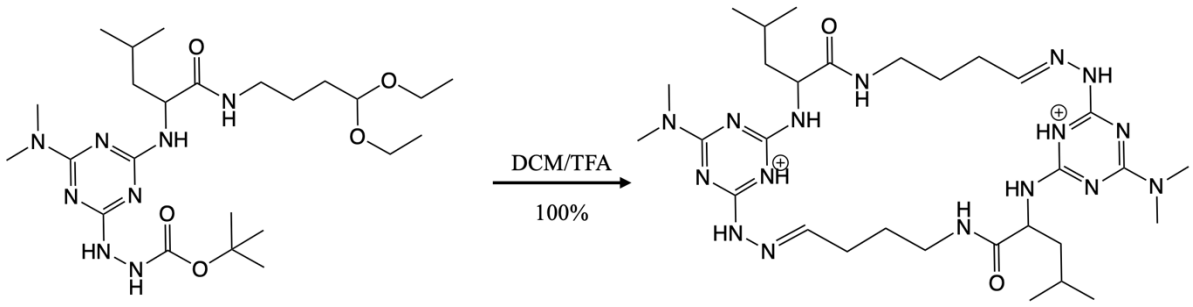

L-Monomer **L-L**

The quantitative yield for this reaction is thought to result from a system of hydrogen bonds that place reactive ends in close proximity in the presence of acid.[7] These interactions create a *zipper effect* (**Figure 2)**. After the first hydrazone forms, hydrogen bonding organizes the other half of the macrocycle in an optimal position for reaction to occur. This positioning prevents the formation of side products or polymers.

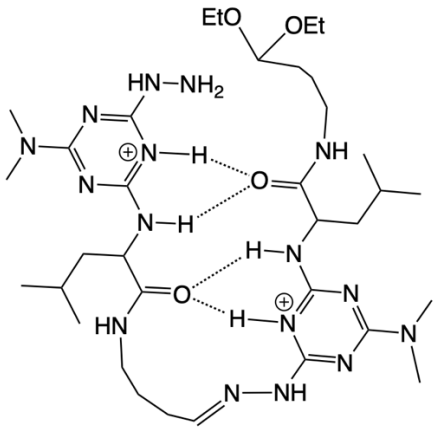

Figure 2. The **L-L** macrocycle highlighting intramolecular "zipper" model.

Macrocycle **L-L** is particularly interesting as leucine side chains are implicated in *beta*-sheet formation common to many protein-protein recognition events. That is, they are commonly found in PPIs, including leucine zippers.[8] Leucine is also predicted to affect the hydrophobicity of this molecule, but the magnitude of this affect is unknown.

To confirm the formation of **L-L** macrocycle, ^{1}H NMR and ^{13}C NMR were used to determine the molecule's structure. To determine whether the macrocycle remained in a planar *beta*-sheet conformation, two-dimensional COSY and rOesy NMR spectra were taken. These spectra allowed for a prediction of the folding properties of these macrocycles. The following pages explore this data and its interpretation.

EXPERIMENTAL

NMR Spectroscopy. NMR spectra (1D and 2D) were recorded using a 400 MHz Bruker Avance spectrometer. Chemical shifts were associated with corresponding solvent peaks.

General Chemistry. Column chromatography was utilized to acquire pure compounds for analysis. All procedures were carried out utilizing reagent grade solvents. Mixtures of MeOH and DCM were utilized for chromatographic purification. Silica gel was utilized with a porosity of 60 Angstroms, particle size 50-63 micrometers, surface area of 500-600 m^2/g, bulk density of 0.4 g/mL, and pH range of 6.5-7.5. Thin-layer chromatography (TLC) was used for assessing the progression of reactions and to ensure the formation of material in a spot-to-spot fashion. Product spots were visualized utilizing either UV light or through ninhydrin staining and the addition of heat. Excess solvents were evaporated from samples using a rotary evaporation.

L-Acid. In a 50 mL round bottom flask, cyanuric chloride (184 mg, 1 mmol) was added to 3 mL of tetrahydrofuran (THF) cooled to -10 ºC in an ice bath of acetone and dry ice. BOC-hydrazine (132 mg, 1 mmol) was dissolved in 3 mL of THF and added dropwise using an addition funnel. One mL of 1M NaOH was added dropwise through the same addition funnel. After 45 minutes TLC in a 9:1 solution of DCM and MeOH showed a single spot with a restriction factor (Rf) of 0.9 under short-wave UV and ninhydrin staining. The reaction mixture was removed from the ice bath. Leucine (262 mg, 2 mmol) was dissolved into a combination of 2 mL water and 3 mL 1M NaOH. This solution was added dropwise via addition funnel into the reaction mixture and was allowed to stir for two hours. TLC using a 9:1 combination of DCM and MeOH indicated a Rf of 0.1 using both short-wave UV and ninhydrin staining. A solution of 40% aqueous dimethylamine (DMA) solution (338 mg, 3 mmol) was added dropwise via pipette and allowed to stir overnight. TLC using a 9:1 combination of DCM and MeOH showed one spot at an Rf of 0.4 in short wave UV and ninhydrin staining. 1M HCl was added into the reaction flask until the pH dropped to 5. The acidified mixture was added to a separatory funnel with equal portions of water and ethyl

acetate. The aqueous layer was then washed with ethyl acetate a subsequent three times. $MgSO_4$ was used to dry the organic layer and was gravity filtered. The solvent was removed using rotary evaporation. The crude product was purified via column chromatography using a 19:1 solution of DCM and MeOH. This yielded 180 mg of pure acid product (47% yield). ^{1}H NMR (DMSO-d_6, 400 MHz): 8.51 (m, 1H), 8.29 (m, 1H), 6.76 (m, 1H), 4.39 (m, 1H), 3.00 (m, 6H), 1.67 (m, 2H), 1.40 (m, 9H), 0.88 (m, 6H). ^{13}C{^{1}H} NMR (DMSO-d_6, 100 MHz): δ 176.0, 168.0, 165.8, 156.5, 150.4, 78.9, 52.6, 39.9, 35.9, 28.6, 24.8, 23.5, 22.1. Results of mass spectrometry analysis are pending.

L-Monomer. **L-**Acid (142 mg, 0.371 mmol) was dissolved into 5 mL of DCM in a reaction flask. Diisopropylethylamine (DIPEA, 135 mg, 0.928 mmol) was added dropwise into the reaction flask. 2-(1H-benzotriazole-1-yl)-1,1,3,3-tetramethyuronium hexafluorophosphate (HBTU, 174 mg, 0.408 mmol) is added as a solid into the reaction flask as the coupling reagent. Finally, 4,4-diethoxybutyl-1-amine (74 mg, 0.408 mmol) was added dropwise over a minute to the reaction flask. The reaction was allowed to proceed overnight. TLC using a 9:1 DCM and MeOH solution had an Rf of 0.6 using both short-wave UV and ninhydrin stain. After the reaction had gone to completion, it was diluted with 15 mL of DCM and added to a separatory funnel. An equivalence of acidified brine was added to wash the organic layer three consecutive times. The organic layer was dried using $MgSO_4$ and solvent was removed using rotary evaporation. The product was then purified utilizing column chromatography with a solvent system of 19:1 DCM and MeOH. This yielded 33 mg of pure product (16.9%). ^{1}H NMR (DMSO-d_6, 400 MHz): 8.49 (m, 1H), 7.73 (m, 1H), 6.63 (m, 1H), 4.43 (m, 1H), 3.52 (m, 1H), 3.41 (m, 1H), 3.00 (m, 6H), 1.40 (m, 6H), 1.31 (s,

1H), 1.09 (m, 6H), 0.87 (m, 6H). $^{13}C\{^{1}H\}$ NMR (DMSO-d_6, 100 MHz): δ 173.5, 168.0, 165.7, 156.5, 102.4, 79.0, 60.9, 53.3, 41.7, 39.9, 38.7, 35.9, 31.1, 28.6, 24.9, 23.6, 22.12, 15.77. Results of mass spectrometry analysis are pending.

Macrocycle L-L. **L**-Monomer (16.6 mg, 0.025 mmol) was dissolved into 1mL of dichloromethane (DCM) in a vial with a stir bar. 1 mL of trifluoroacetic acid (TFA) was added dropwise to the vial. The reaction was left open and allowed to evaporate over a week. The resulting compound was analyzed via NMR spectroscopy. ^{1}H NMR (DMSO-d_6, 400 MHz): 12.6 (s, 1H), 12.4 (s, 1H), 9.74 (m, 1H), 8.48 (m, 1H), 7.91 (s, 2H), 7.58 (m, 1H), 4.48 (m, 1H), 3.13 (d, 6H), 2.84 (m, 2H), 2.39 (m, 2H), 1.82 (m, 2H), 1.67 (m, 3H), 0.92 (m, 6H). $^{13}C\{^{1}H\}$ NMR (DMSO-d_6, 100 MHz): δ 173.5, 162.2, 159.0, 154.0, 152.1, 118.5, 115.5, 112.6, 52.43, 39.9, 38.7, 37.0, 36.9, 29.4, 24.8, 24.1, 23.1, 22.1. Results of mass spectrometry analysis are pending.

RESULTS AND DISCUSSION

Synthesis Pathway: Cyanuric chloride is added into a round bottom flask, followed by the sequential addition of three different substituents to the triazine core (**Scheme 2**). For the acid formation, all reactions progressed in a one-pot synthesis. THF was used as the primary solvent and 1M NaOH as the base for the substitution reactions.

Scheme 2. Synthesis of acid. a) $BOCNHNH_2$, NaOH *(aq)*, THF, -10 ºC, 45 min b) Leu, NaOH *(aq)*, 3 h. c) 40% $HN(CH_3)_2$ *(aq)*, 2 h. d) 4,4-diethoxybutyl-1-amine, HBTU, DIPEA *(aq)* 24 h.

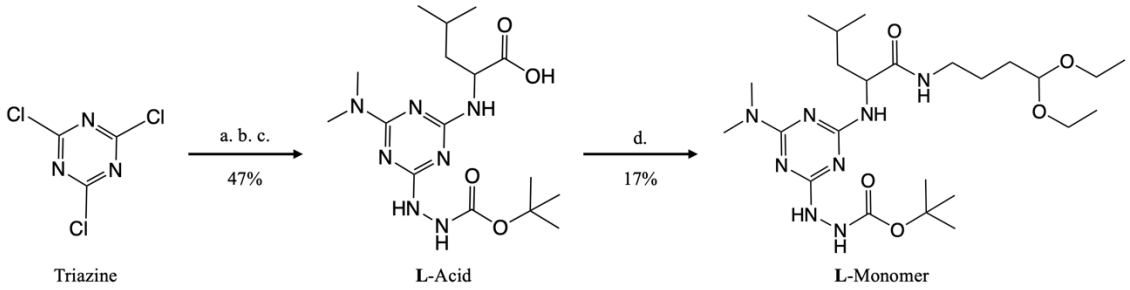

BOC-hydrazine serves as the initial substitution because of its ability to be easily handled and its ability to increase the solubility of the resulting product. The BOC-hydrazine was added at -10 ºC to prevent a double or triple substitution onto the cyanuric chloride. A molar equivalence of the BOC-hydrazine was added to the reaction flask after being dissolved in 5 mL of THF. Subsequently, a molar equivalent of NaOH was added to the reaction flask to facilitate the substitution. The pH of the solution was monitored to ensure that conditions were optimal for substitution.

Leucine was utilized in the second substitution, dissolving two equivalents of amino acid in a solution equal parts water and NaOH and added dropwise to the reaction flask. DMA was the final addition to the cyanuric chloride. Three molar equivalents of a 40% DMA solution were added dropwise to the reaction flask to ensure final product formation.

Each reaction was monitored utilizing thin layer chromatography to ensure the reactions proceeded in a "spot-to-spot" manner. To isolate the acid, the reaction flask was acidified using 1M HCl to a pH of approximately 5. The reaction mixture was then added to a separatory funnel with an equivalent amount of brine and ethyl acetate. The aqueous layer was washed four times with equivalent additions of ethyl acetate. The resulting organic layer was dried utilizing $MgSO_4$ and was gravity filtered before being rotary evaporated, resulting in a crude product in the form of a white powder. The product was purified utilizing column chromatography with a 19:1 ratio of DCM and MeOH. This results in the formation of the leucine acid, **L**-acid. The result was 180 mg of pure acid, a 47% yield.

To characterize the acid, 40 mg of the pure product was dissolved in DMSO-d_6 and was analyzed utilizing a ^{1}H-NMR (**Figure 3)**. Each substitution on the triazine core has a unique and characteristic peak within the NMR spectra which confirms that synthesis was successful, and that the resulting product is pure. In addition, the number of protons associated with each resonance corroborates the conclusion.

The BOC-group appears as a sharp singlet near 1.40 ppm with an integration consistent with the three methyl groups present. This addition is also confirmed through the appearance of peaks at 8.5 ppm indicative of the hydrazine and labeled as NHNH. The leucine substitution results in apparent aliphatic peaks that are farther upfield indicated with α, β, γ, and δ with the associated nitrogen being labeled as α-NH appearing downfield. Specifically, the α peak near 4.2 ppm the α-NH peak downfield confirms the addition of leucine to the acid. The appearance of multiple α and

α-NH peaks can be explained by the formation of rotamers in solution. DMA addition is confirmed through the appearance of two singlets at 3.01 ppm.

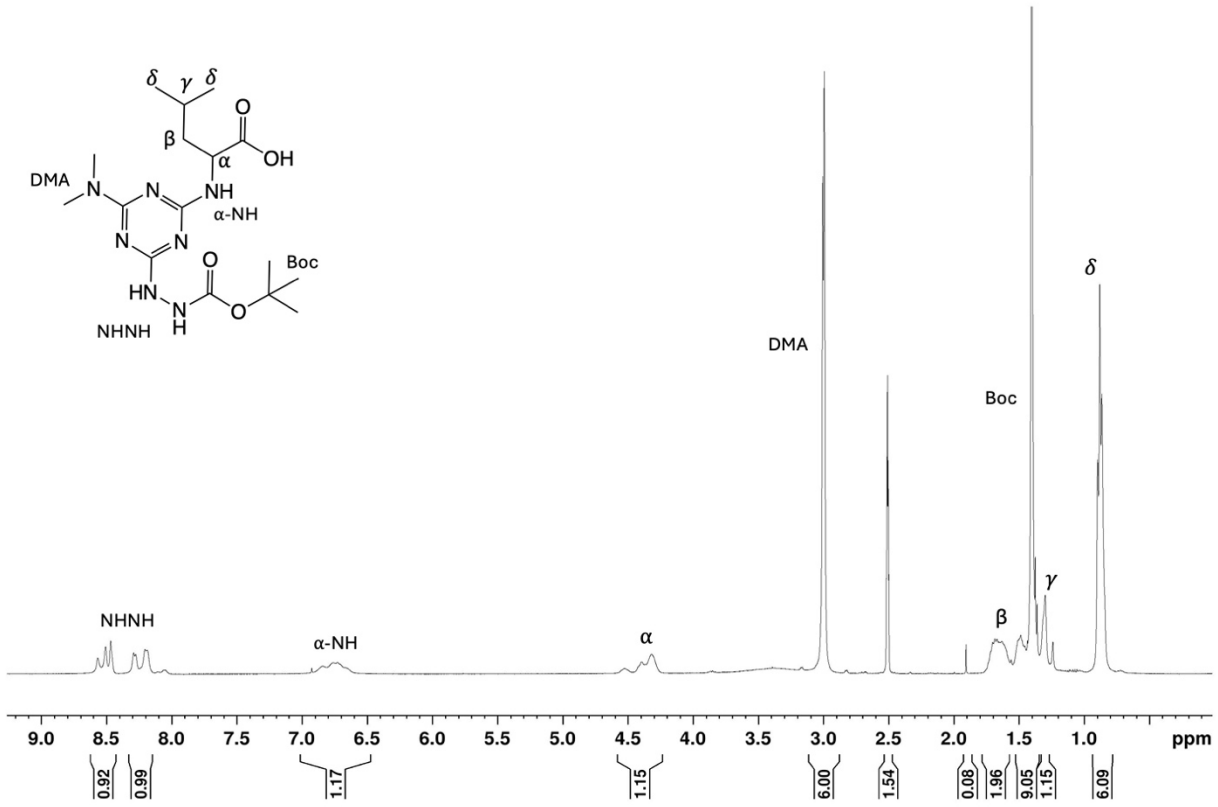

Figure 3. The 400 MHz ^{1}H NMR spectrum of **L-**acid in DMSO-d_6

The ^{13}C NMR of the **L-**Acid provides additional confirmation that the **L-**Acid has formed (**Figure 4**). Peaks can be assigned in the spectra by predicting the different electron environments of the carbon atoms. Electron-rich carbons are associated with upfield peaks at lower ppm while electron-poor carbons are indicated by peaks at higher ppm. The three downfield resonances from 150-180 ppm are indicative of three substitutions on the triazine ring, confirming the attachment of all three substituents.

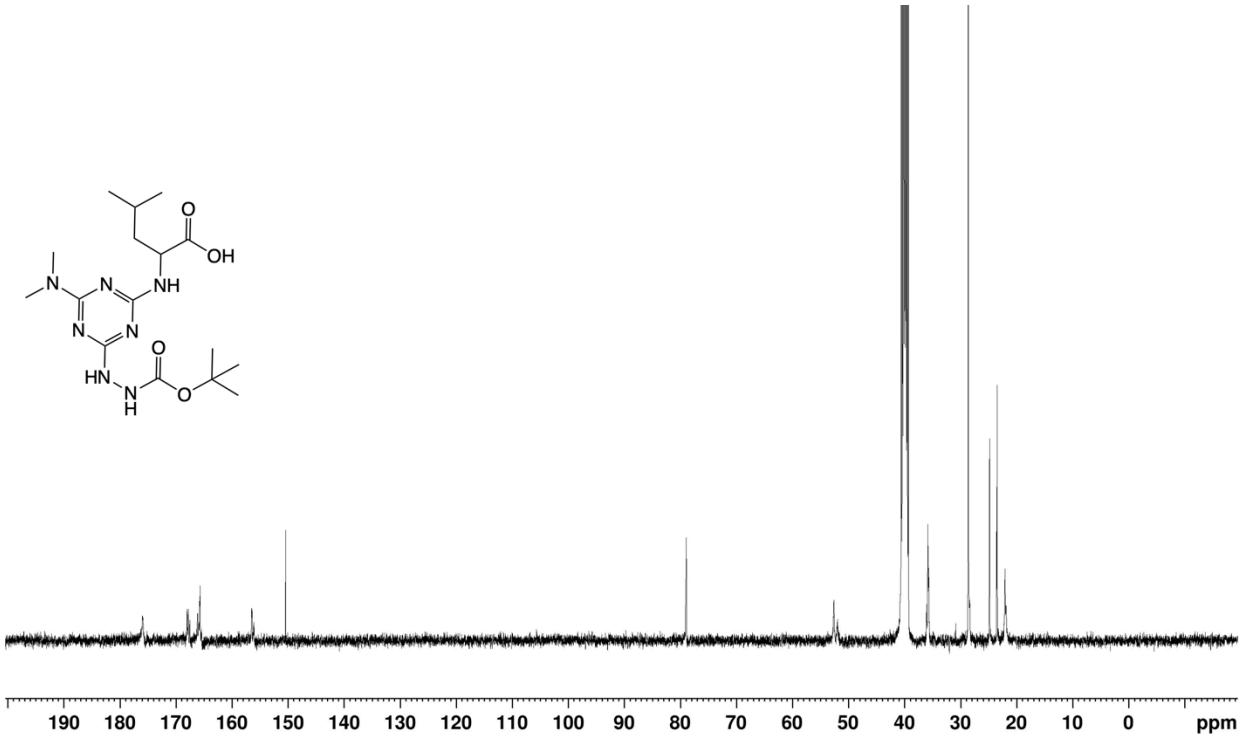

Figure 4. The 100 MHz ^{13}C NMR spectrum of **L-**acid in DMSO-d_6

After the formation of the acid is confirmed, installation of the four-carbon acetal is performed using HBTU as a coupling agent and a molar equivalent of DIPEA as a base. The reaction mixture is dissolved in equivalent amounts of ethyl acetate and brine. The organic layer is washed using multiple additional measures of brine. The resulting monomer is then purified utilizing column chromatography with a 19:1 solution of DCM and MeOH. After purification, 33 mg of monomer was collected, a 17% yield.

The composition of the **L-**Monomer was confirmed utilizing ^{1}H-NMR which showcased the appearance of A, B, C, and D peaks as well as peaks characteristic of ethyl groups labeled as -OCH_2 and -CH_3 (**Figure 5**). The -OCH_2 group appears at 3.54 and 3.39 ppm as multiplets and the -CH_3 groups are evident as a peak near 1.10 ppm. The other carbons of the acetal appear upon a

continuum ranging from 1.5 to 4.5 ppm. The A peak at 4.5 ppm is of particular interest as it plays a vital role in the conformation of cyclization.

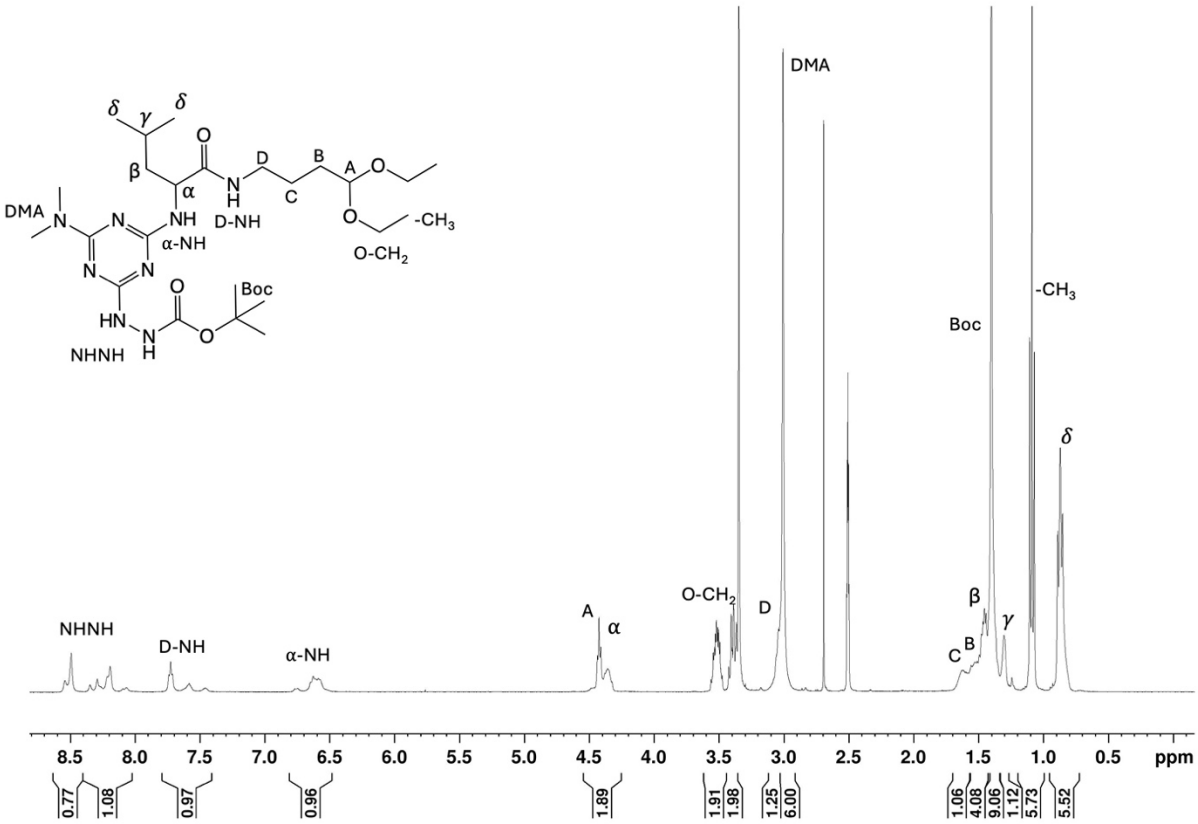

Figure 5. The 400 MHz ^{1}H NMR spectrum of **L-**monomer in DMSO-d_6

The ^{13}C NMR of the **L-**Monomer further supports that the acetal installation has occurred and that the **L-**Monomer product is pure **(Figure 6**). The appearance of a peak near 100 ppm corresponds to the acetal carbon. The presence of this resonance confirms the formation of the **L-**Monomer.

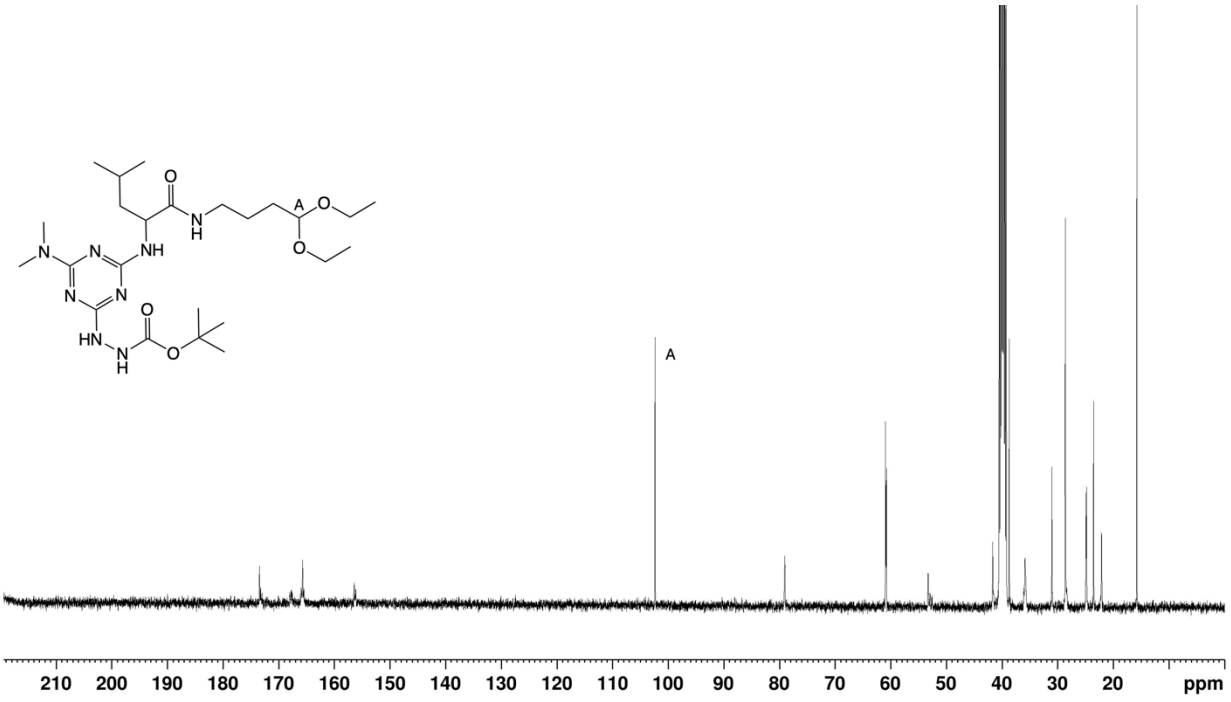

Figure 6. The 100 MHz ^{13}C NMR spectrum of **L-**monomer in DMSO-d_6

*Synthesis and Structural Characterization of **L-L**.* Synthesis of macrocyclic compounds has been found to proceed in a quantitative yield without the need for purification. Monomer is added to a 10 mL vial with a 1:1 mixture of DCM and TFA. The vial is left uncapped with a stir bar to allow for solvent evaporation over seven days. After the evaporation of the solvent, the resulting macrocycle can be characterized using NMR analysis with macrocycle dissolved in DMSO-d_6.

The ^{1}H-NMR spectrum of the macrocycle confirms successful synthesis, and that the reaction went to completion (**Figure 7)**. The loss of resonances for the BOC protecting group and the loss of resonances associated with the acetal ethyl groups are particularly helpful in identifying that the reaction has gone to completion and that macrocycle formation has occurred. In addition to the

loss of resonances, the appearance of resonances corresponding to the newly formed hydrazone and the downfield shift of the A peak further confirm that synthesis has been successful.

There is also support for the proposed hydrogen bonding structure of the **L-L** macrocycle. The downfield shift of resonances associated with the α-NH, NNH, H^+, and D-NH peaks indicates that the associated protons are further deshielded, which can be explained through intramolecular hydrogen bonding. These shifts are consistent with the hydrogen bond scaffold seen in the macrocycle structure and offer the most compelling evidence that a structure resembling a *beta*-sheet is adopted.

The ^{13}C NMR spectra of the **L-L** macrocycle also confirms cyclization (**Figure 8**). The disappearance of the acetal peak at 100 ppm indicates that this group has been removed. In addition, the appearance of a new peak downfield at 158 ppm is indicative of the symmetric hydrazone formation.

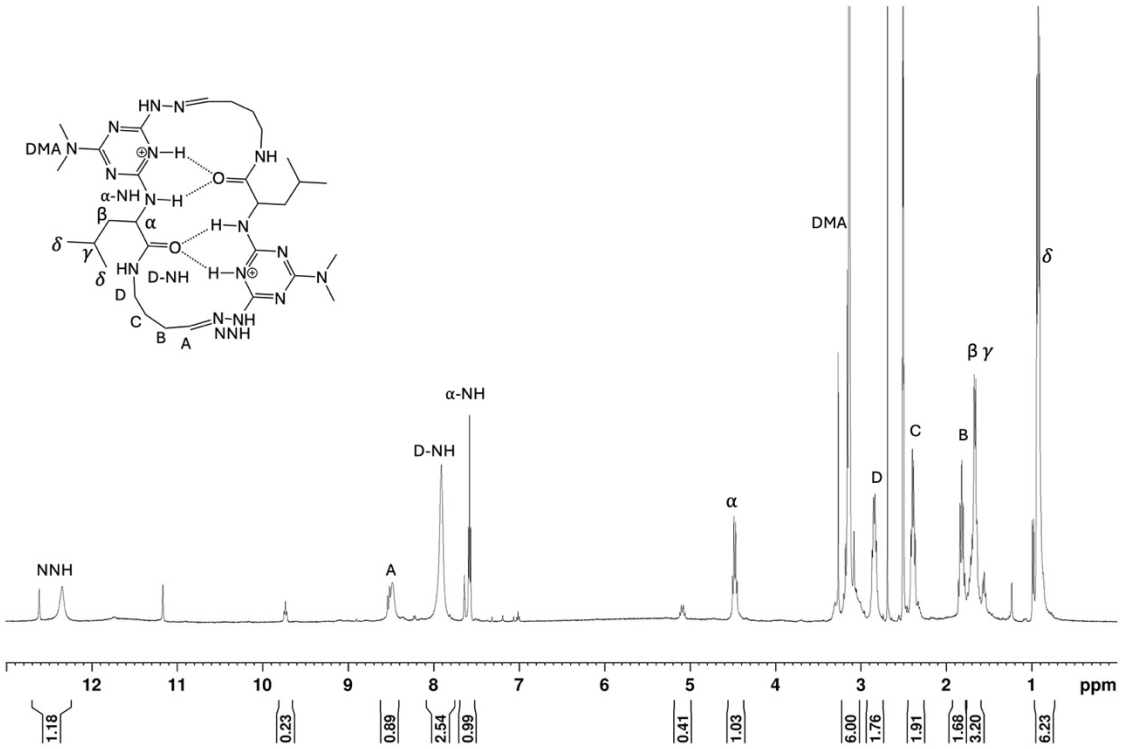

Figure 7. The 400 MHz ^{1}H NMR spectrum of **L-L** macrocycle in DMSO-d_6

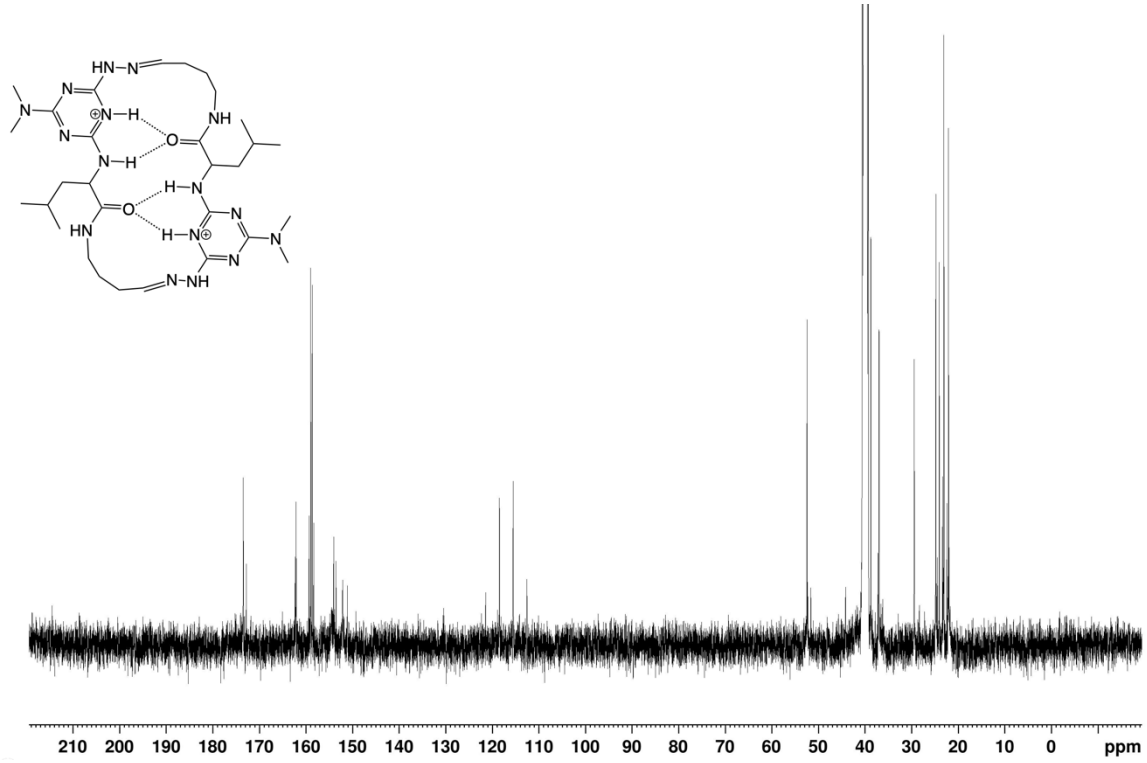

Figure 8. The 100 MHz ^{13}C NMR spectrum of **L-L** macrocycle in DMSO-d_6

Characterization of macrocycle shape. The utilization of two-dimensional NMR spectra works to confirm the primary structural conformation of the **L-L** macrocycle. A COSY experiment is utilized to show correlations between hydrogens on adjacent carbons (**Figure 9)**. COSY spectra visualize hydrogen interactions between hydrogens that are on the immediate carbon. Correlations seen on the spectra indicate that the hydrogens associated with those peaks are attached to adjacent atoms. This correlation offers a way to confirm the assignment of peaks within the macrocycle in ^{1}H-NMR. Determining the correlations between peaks is essential to understanding the primary structure of the molecule and confirm the location of each atom within the macrocyclic ring.

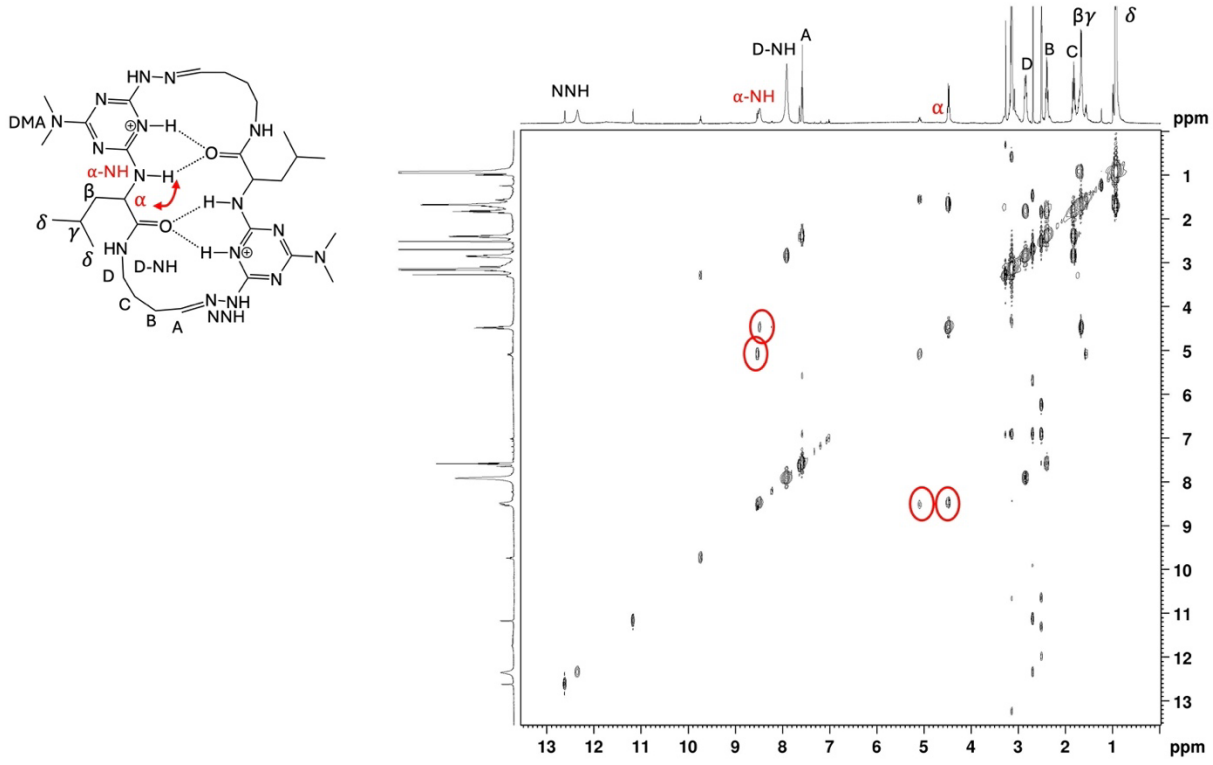

Figure 9. The COSY spectra of the **L-L** 26-atom macrocycle. Circles indicate correlations between hydrogens on adjacent carbons.

The COSY spectra confirms that the peaks of the ^{1}H-NMR have been properly assigned. This experiment can be understood by observing the correlations between different NMR peaks. For example, the correlations between the D-NH and D peaks confirm that the one-dimensional NMR peaks have been properly assigned. If these correlations were not present, it would be indicated that there is a significant distance between the hydrogens related to those peaks and support a different assignment of hydrogens on the macrocycle. This spectra also indicates that there may be a certain amount of splitting in certain peaks such as the alpha peak, indicated with red circles. This splitting can be indicative of impurities within the sample or can be a result of conformational changes in the folding of the macrocycle.

To identify the shape of this macrocycle, a rOesy experiment is utilized to identify hydrogens that see each other across space. This type of two-dimensional NMR analysis looks at hydrogens that see each other at a set distance, unrelated to their linkages. This property allows for identification of structural conformation by revealing the cross talk between different protons on the macrocycle. In a folded conformation, we expect a cross correlation between the DMA methyl group and the proton associated with carbon A which has been seen in previously synthesized macrocycles (**Figure 10).**

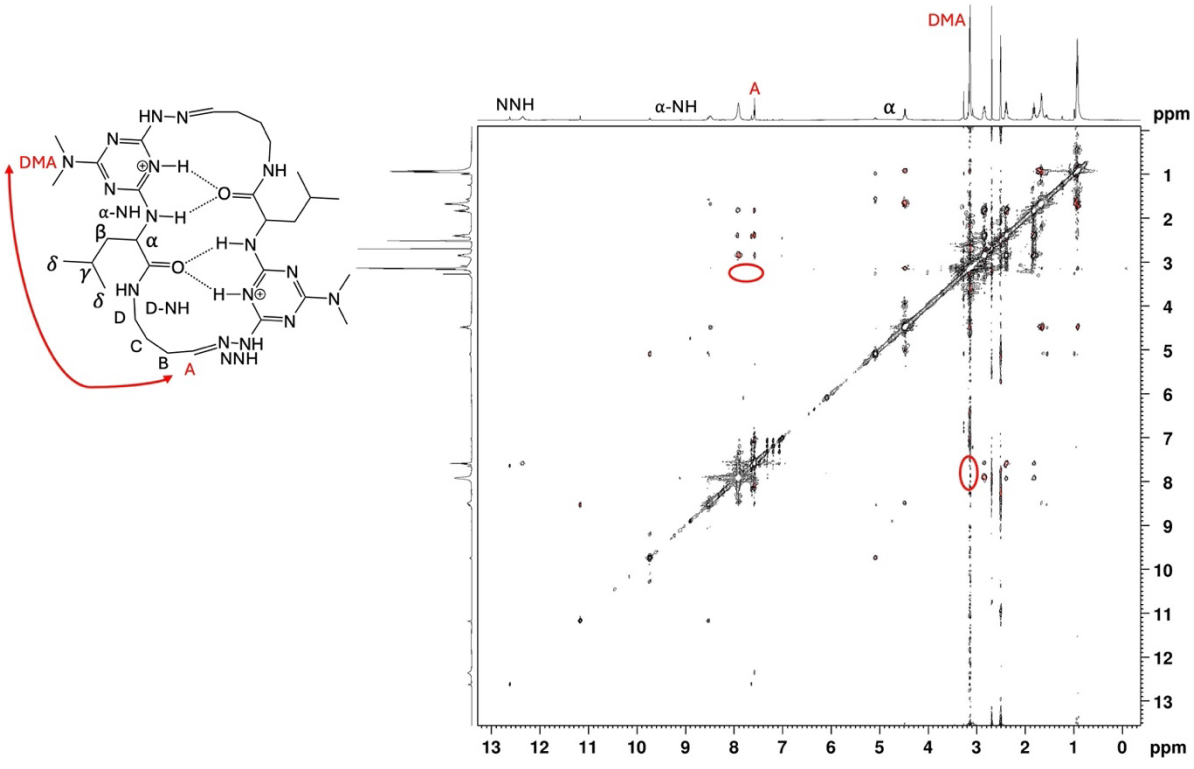

Figure 10. rOesy spectra of the **L-L** macrocycle, highlighting the lack of cross peaks between the DMA and A peaks of the macrocycle.

The lack of correlation between the DMA and A hydrogens supports that the **L-L** macrocycle maintains a planar conformation, comparable to the **G-G** macrocycle previously recorded. While the absence of a correlation does indicate that the planar conformation is maintained, as seen in the **G-G** macrocycle, **Figure 1**, additional testing would be needed to provide sufficient evidence. X-ray crystallography would be a logical next step in understanding and confirming the structural status of the **L-L** 26-atom macrocycle.

CONCLUSION

The 26-atom macrocycle, **L-L**, is available in three steps. The addition of BOC-hydrazine, leucine, and DMA offers the **L-**Acid at a yield of 47%. Coupling with a four-carbon acetal occurs at a yield of 16.9% and generates the formation of the **L-**Monomer. Cyclization of the monomer into the resulting **L-L** macrocycle occurs in a 100% yield after the addition of TFA and DCM. ^{1}H NMR is utilized to confirm the structure of each intermediate and resulting macrocyclic compound. Based on the rOesy experimentation, there is evidence to support the maintenance of a planar *beta*-sheet conformation found in the **G-G** macrocycle after the substitution with large non-polar amino acid groups. The downfield shifts of α-NH and D-NH between the **L-**Monomer and the **L-L** macrocycle ^{1}H-NMR spectra is also consistent with the proposed hydrogen bonding network.

The lack of rOesy correlations between DMA and A peaks in the macrocycle rOesy experiment indicates that there is no folding of the molecule. However, there is also no positive provocative indicator confirming that folding is not taking place. To confirm that the conformation is still planar future experimentation including X-ray crystallography must be utilized.

In addition, the formation of planar sheets has not been analyzed after the addition of polar or charged amino acids, which could alter the structural conformation of the molecule. Synthesis of a molecular library of 26-atom macrocycles could offer greater insight into the effects of different substitutions on the overall structure of macrocyclic molecules.

Support of the maintenance of planar conformation in the **L-L** 26-atom macrocycle is valuable as it highlights how structure can be predicted in macrocycle formation. Structure plays a significant role in pharmaceutical design and bioavailability. Because of the maintained *beta*-sheet conformation there is support for further exploration into molecularly analogous structures that could be formed utilizing macrocycles.

REFERENCES

1. Sharma, Vishal R., et al. “Efficient syntheses of macrocycles ranging from 22–28 atoms through spontaneous dimerization to yield bis-hydrazones.” *RSC Advances*, **2020**, 10 (6), 3217–3220, DOI: 10.1039/c9ra08056b

2. Müller, R.H., et al. “Oral bioavailability of cyclosporine: Solid lipid nanoparticles (SLN®) versus Drug Nanocrystals.” *Int. J. Pharm.,* **2006**, 317 (1), 82–89, DOI: 10.1016/j.ijpharm.2006.02.045.

3. Yepremyan, Akop, et al. “Synthesis of macrocycles derived from substituted triazines.” *ChemBioChem*, **2018**, 20 (2), 241–246, DOI: 10.1002/cbic.201800475.

4. Menke, Alexander J., et al. “A model for the rapid assessment of solution structures for 24-atom macrocycles: The impact of β-branched amino acids on conformation.” *J. Org. Chem.,* **2023**, 88 (5), 2692–2702, DOI: 10.1021/acs.joc.2c01984.

5. Shultz, Michael D. “Two decades under the influence of the rule of five and the changing properties of approved oral drugs.” *J. Med. Chem.,* **2018**, 62 (4), 1701–1714, DOI: 10.1021/acs.jmedchem.8b00686.

6. Laxio Arenas, José, et al. “Peptides and peptidomimetics as inhibitors of protein–protein interactions involving β-sheet secondary structures.” *COCHBI,* **2019**, 52, 157–167, DOI: 10.1016/j.cbpa.2019.07.008.

7. Menke, A. J., Henderson, N. C., Kouretas, L. C., Estenson, A. N., Janesko, B. G., & Simanek, E. E. “Computational and experimental evidence for templated macrocyclization: The role of a hydrogen bond network in the quantitative dimerization of 24-atom macrocycles”. *Molecules*, **2023,** 28 (3), 1144, https://doi.org/10.3390/molecules28031144

8. Chou, Peter Y., and Gerald D. Fasman. “Structural and functional role of leucine residues in proteins.” *J. Mol. Biol.,* **1973**, 74 (3), 263–281, DOI: 10.1016/0022-2836(73)90372-0.